Histone demethylase JMJD1A promotes alternative splicing of AR variant 7 (AR-V7) in prostate cancer cells

Lingling Fan[a,b,1], Fengbo Zhang[a,b,c,1], Songhui Xu[a,b], Xiaolu Cui[a,b], Arif Hussain[b,d], Ladan Fazli[e], Martin Gleave[e], Xuesen Dong[e], and Jianfei Qi[a,b,2]

[a]Department of Biochemistry and Molecular Biology, University of Maryland School of Medicine, Baltimore, MD 21201; [b]Marlene and Stewart Greenebaum Comprehensive Cancer Center, Baltimore, MD 21201; [c]Department of Urology, Beijing Friendship Hospital, Capital Medical University, Beijing 100050, China; [d]Baltimore VA Medical Center, Baltimore, MD 21201; and [e]Vancouver Prostate Centre, University of British Columbia, Vancouver, BC V6H 3Z6, Canada

Edited by Owen N. Witte, University of California, Los Angeles, CA, and approved April 6, 2018 (received for review February 8, 2018)

Formation of the androgen receptor splicing variant 7 (AR-V7) is one of the major mechanisms by which resistance of prostate cancer to androgen deprivation therapy occurs. The histone demethylase JMJD1A (Jumonji domain containing 1A) functions as a key coactivator for AR by epigenetic regulation of H3K9 methylation marks. Here, we describe a role for JMJD1A in AR-V7 expression. While JMJD1A knockdown had no effect on full-length AR (AR-FL), it reduced AR-V7 levels in prostate cancer cells. Reexpression of AR-V7 in the JMJD1A-knockdown cells elevated expression of select AR targets and partially rescued prostate cancer cell growth in vitro and in vivo. The AR-V7 protein level correlated positively with JMJD1A in a subset of human prostate cancer specimens. Mechanistically, we found that JMJD1A promoted alternative splicing of AR-V7 through heterogeneous nuclear ribonucleoprotein F (HNRNPF), a splicing factor known to regulate exon inclusion. Knockdown of JMJD1A or HNRNPF inhibited splicing of AR-V7, but not AR-FL, in a minigene reporter assay. JMJD1A was found to interact with and promote the recruitment of HNRNPF to a cryptic exon 3b on AR pre-mRNA for the generation of AR-V7. Taken together, the role of JMJD1A in AR-FL coactivation and AR-V7 alternative splicing highlights JMJD1A as a potentially promising target for prostate cancer therapy.

histone demethylase | JMJD1A | androgen receptor | RNA splicing | prostate cancer

Androgen deprivation therapy (ADT), which blocks androgen receptor (AR) activity, is the primary treatment for metastatic prostate cancer. Despite an initially beneficial response to ADT, a majority of patients with prostate cancer eventually become resistant to such therapies and progress to castration-resistant prostate cancer (CRPC), which is an incurable and ultimately lethal disease state. Activation of AR signaling despite low androgen levels is believed to underlie the development of CRPC in most cases (1, 2).

Restoration of AR transcriptional activity in CRPC can occur through a variety of mechanisms, among which is the formation of AR splicing variants (AR-Vs) (3–5). Full-length AR (AR-FL) consists of an N-terminal transactivation domain (N-TAD), a DNA-binding domain (DBD), a hinge region, and a C-terminal ligand-binding domain (LBD). Although AR-Vs lack an LBD, they drive the AR transcriptional program in a constitutively active manner. AR-V7 (also called AR3) is one of most widely studied AR variants. Expression of AR-V7 is associated with resistance to AR signaling inhibitors and poor prognosis of prostate cancer (6, 7). The AR gene consists of eight exons that encode different regions: exon 1 encodes N-TAD, exons 2 and 3 encode the DBD, and exons 4–8 encode the hinge region and LBD. AR-FL and AR-V7 are derived from the same AR pre-mRNA through alternative splicing. In contrast to AR-FL mRNA that includes all eight exons, AR-V7 is generated via use of a cryptic exon 3b located in the third intron of AR, which results in the formation of AR-V7 mRNA that only includes exons 1–3 and 3b (4, 5). The various AR-Vs can form homodimers among themselves or heterodimers with AR-FL to transcribe target genes (8–10). The target genes regulated by AR-FL and AR-V7 overlap but are not identical (4, 11, 12). The role of AR-V7 in transcriptional regulation and CRPC progression has been extensively studied. However, the mechanisms controlling the alternative splicing of AR pre-mRNA to generate AR-V7 remain poorly explored.

JMJD1A (Jumonji domain containing 1A; i.e., KDM3A) is a histone demethylase that removes the repressive H3K9 methylation marks (H3K9me1 or H3K9me2) to regulate gene expression (13, 14). We previously reported that JMJD1A played a key role in the proliferation and survival of prostate cancer cells, in part, through regulation of the AR transcriptional program and elevation of c-Myc levels (15, 16). JMJD1A interacts with AR and functions as a key AR coactivator through its histone demethylase activity (13, 15). This study reveals a role for JMJD1A in the alternative splicing of AR pre-mRNA to generate AR-V7.

Splicing of mRNA is performed by the spliceosome, a large complex of proteins and snRNAs that recognizes specific sequence elements within an intron (e.g., 5′ splice site, 3′ splice site), removes the intron, and ligates the adjacent exons. The splicing factors, which bind to specific sequence elements on pre-mRNAs and promote exon inclusion or skipping, regulate the efficiency of splice site recognition by the spliceosome. Heterogeneous nuclear ribonucleoprotein F (HNRNPF) and highly related HNRNPH are splicing factors that bind to the guanosine (G)-rich sequence in exons or introns, and thus function as either enhancers or inhibitors of alternatively spliced exons (17–21). In

Significance

Formation of androgen receptor splicing variant 7 (AR-V7), a constitutively active form of AR, plays a key role in the resistance of prostate cancer to hormone therapy. However, the mechanisms that regulate AR-V7 generation are poorly understood. Here, we identified a new role for histone demethylase JMJD1A (Jumonji domain containing 1A) in the formation of AR-V7 in prostate cancer cells. We found that JMJD1A facilitated recruitment of a splicing factor, heterogeneous nuclear ribonucleoprotein F, for alternative splicing and generation of AR-V7. The findings suggest that targeting JMJD1A may provide new therapeutic opportunity for prostate cancer.

Author contributions: J.Q. designed research; L. Fan, F.Z., S.X., X.C., and L. Fazli performed research; A.H., M.G., and X.D. contributed new reagents/analytic tools; L. Fazli and J.Q. analyzed data; and J.Q. wrote the paper.

The authors declare no conflict of interest.

This article is a PNAS Direct Submission.

[1]L. Fan and F.Z. contributed equally to this work.

[2]To whom correspondence should be addressed. Email: jqi@som.umaryland.edu.

This article contains supporting information online at www.pnas.org/lookup/suppl/doi:10.1073/pnas.1802415115/-/DCSupplemental.

Published online April 30, 2018.

this study, we found that JMJD1A interacts with HNRNPF and promotes the recruitment of HNRNPF to exon 3b of AR pre-mRNA, resulting in its splicing to create the AR-V7 variant.

Results

JMJD1A Knockdown Reduces the Level of AR-V7 in Prostate Cancer Cells. JMJD1A is a key AR coactivator in prostate cancer cells (15, 16). To examine the effect of androgens on JMJD1A and AR, we switched CWR22Rv1 prostate cancer cells (hereafter called Rv1 cells) to growth media containing 5% charcoal-stripped FBS (which has low androgen levels) and supplemented the media with either 5 μM antiandrogen enzalutamide (to maximally block androgenic action) or 1 nM synthetic androgen R1881 (to restore androgens to physiological levels). The former mimics androgen deprivation conditions, while the latter reflects normal androgen conditions. We found that protein levels of JMJD1A and AR-FL in Rv1 cells were not affected irrespective of the androgen conditions (Fig. 1*A*). Interestingly, although knockdown of JMJD1A in Rv1 cells had little effect on the protein levels of AR-FL, we found reduced levels of a protein band at 80 kDa, which is consistent with the size of AR-Vs (Fig. 1*A*). Using an AR-V7 specific antibody, Western blot analysis demonstrated that JMJD1A knockdown indeed reduced the protein levels of AR-V7 in Rv1 cells (Fig. 1*A*). Furthermore, qRT-PCR analysis showed that JMJD1A knockdown in Rv1 cells reduced mRNA levels of AR-V7, but not AR-FL, under either androgen-deprived or normal conditions (Fig. 1*B*).

LN95 and VCaP are two other prostate cancer cell lines known to express AR-V7, albeit at lower levels than Rv1 cells (Fig. S1*A*). Similar to our findings with Rv1 cells, JMJD1A knockdown in LN95 cells reduced mRNA levels of AR-V7, but not AR-FL, under both normal and androgen-deprived conditions (Fig. 1*C*). Unlike Rv1 or LN95 cells, mRNA levels of both AR-FL and AR-V7 were up-regulated in VCaP cells upon androgen deprivation (Fig. 1*D*), likely due to the transcriptional up-regulation of AR pre-mRNA in this cell line (22, 23). Nonetheless, JMJD1A knockdown in VCaP cells reduced mRNA levels of AR-V7, but not AR-FL, under either androgen deprivation or normal conditions (Fig. 1*D*). Taken together, these results indicate that JMJD1A promotes the expression of AR-V7, but not AR-FL, in prostate cancer cells known to express AR-V7.

To confirm the relevance of our findings to human prostate cancer, we evaluated the expression of JMJD1A and AR-V7 in a

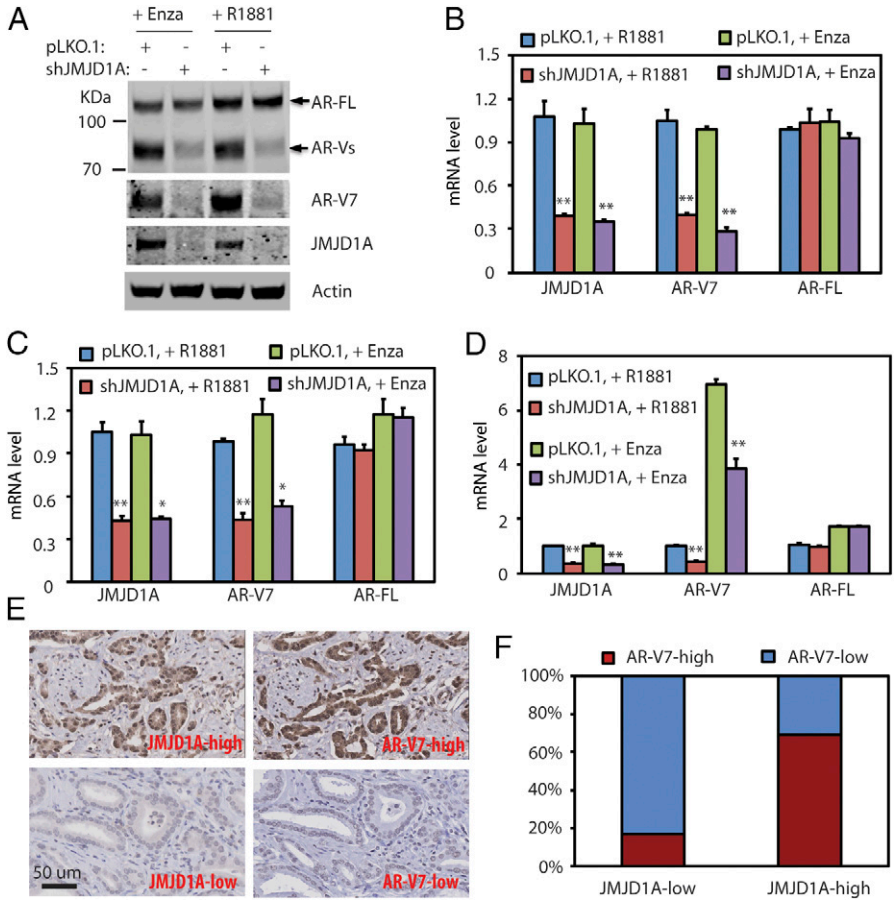

Fig. 1. (*A*) Rv1 cells were transduced with pLKO.1 control or JMJD1A shRNAs for 24 h. Then, cells were maintained in growth media that contained 5% charcoal-stripped-FBS supplemented with either enzalutamide (Enza; 5 μM) or R1881 (1 nM). After 24 h, cell lysates were collected for Western blot analyses using the indicated antibodies. (*B*) Rv1 cells described in *A* were analyzed by qRT-PCR for transcripts of JMJD1A, AR-V7, or AR-FL. (*C*) LN95 cells (pLKO.1 or JMJD1A-knockdown) were treated and analyzed by qRT-PCR as described in *A* and *B*. (*D*) VCaP cells (pLKO.1 or JMJD1A-knockdown) were treated and analyzed by qRT-PCR as described in *A* and *B*. In *B*–*D*, the comparison with statistical significance (pLKO.1 vs. shJMJD1A) is indicated with an asterisk (**$P < 0.01$, *$P < 0.05$; ANOVA). (*E*) Immunohistochemistry staining of JMJD1A or AR-V7 was performed on prostate cancer TMA. The staining was developed with DAB (brown) and counterstained with hematoxylin (blue). Shown are representative images of high (*Upper*) and low (*Lower*) levels of JMJD1A or AR-V7 staining. (*F*) Quantification of JMJD1A or AR-V7 staining of prostate cancer TMA ($n = 40$). The staining of JMJD1A or AR-V7 was scored as 3 (strong), 2 (moderate), 1 (weak), or 0 (none). Scores of 3 or 2 were defined as high, and scores of 1 or 0 were defined as low. The Mann–Whitney *U* test was used for statistical analysis ($P < 0.01$).

human prostate cancer tissue microarray (TMA) containing tumor samples of Gleason grades 3–5. JMJD1A and AR-V7 staining revealed primarily nuclear localization, but varying degrees of cytoplasmic staining of both proteins were also observed in some samples (Fig. 1*E*). Based on the relative staining intensity, we defined AR-V7 staining as either high (strong or moderate) or low (weak or none). JMJD1A staining was likewise defined as either high or low. Approximately 69.2% of JMJD1A-high tumors exhibited high staining of AR-V7, whereas only 16.7% of JMJD1A-low tumors exhibited high staining of AR-V7, with the majority (83.3%) stained at low intensity (Fig. 1*F*). These results indicate that JMJD1A may also promote the expression of AR-V7 in a subset of human prostate cancer tissues.

We previously reported that JMJD1A knockdown reduced levels of c-Myc in prostate cancer cells (15). To evaluate the possible involvement of c-Myc in modulating AR-V7 expression, we knocked down c-Myc in Rv1, LN95, and VCaP cells but found no change in AR-V7 mRNA levels (Fig. S1*B*). This indicates that c-Myc does not affect AR-V7 expression in these prostate cancer cell lines.

JMJD1A Promotes the Expression of Select AR Targets Through AR-V7. JMJD1A is known to interact with and coactivate AR-FL in prostate cancer cells (13, 15). To assess if JMJD1A also interacts with AR-V7, we coexpressed myc-JMJD1A with either Flag-tagged AR-FL or AR-V7 in 293T cells and performed immunoprecipitation studies using anti-Flag M2 beads. Myc-JMJD1A coprecipitated with Flag-AR-FL, but not with Flag-AR-V7 (Fig. 2*A*), indicating that JMJD1A does not directly interact with AR-V7, and thus may not function as its coactivator. Of note, AR-FL and AR-V7 were shown to regulate the expression of both common and unique AR targets (4, 11, 12). If this were true, we reasoned that restoration of AR-V7 expression in JMJD1A-knockdown Rv1 cells should be able to rescue expression of AR targets that depend on AR-V7. To determine the dependency of AR targets on AR-FL or AR-V7, we knocked down AR-FL using shRNA that targeted the AR LBD domain and

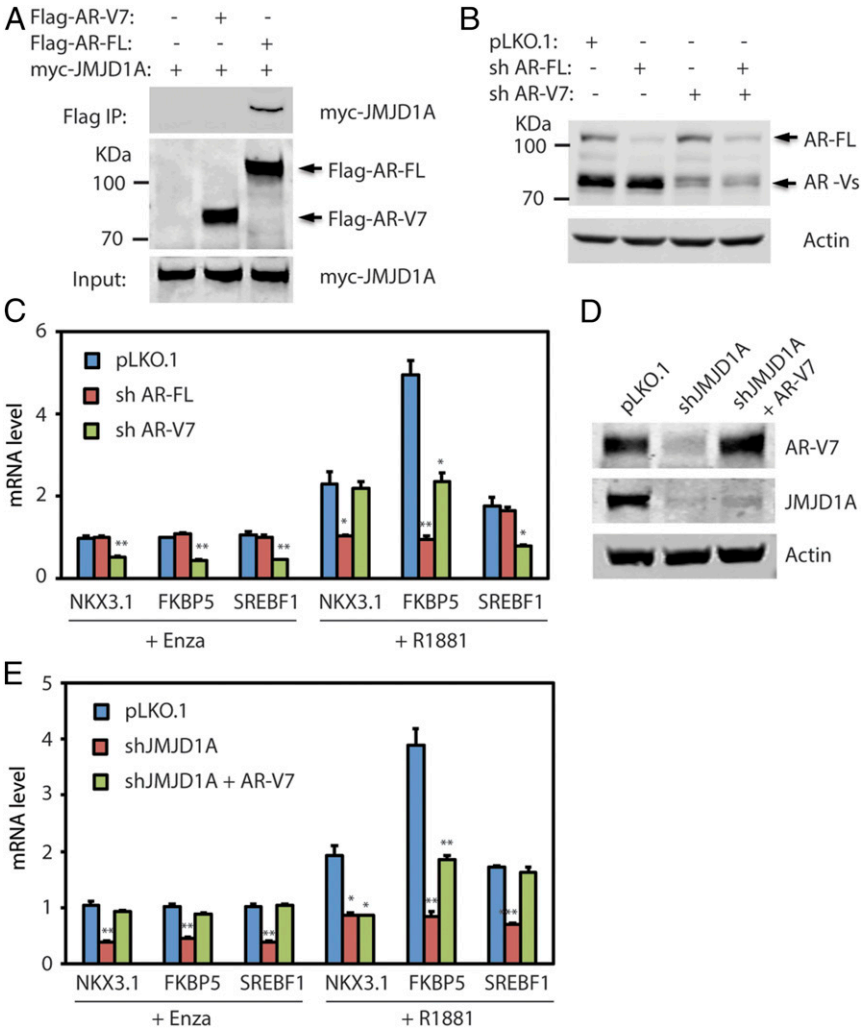

Fig. 2. (*A*) Flag-tagged AR-V7 or AR-FL was cotransfected with myc-JMJD1A in 293T cells for 24 h. Cell lysates were then subjected to immunoprecipitation (IP) with anti-Flag M2 beads. Bound proteins were analyzed by Western blotting with myc or Flag antibodies. (*B*) Rv1 cells were transduced with pLKO.1 control, AR-V7 shRNA, or AR-FL shRNA. After 48 h, cell lysates were analyzed by Western blotting with the AR antibody (N-20) that recognizes the AR N-terminal region. (*C*) Rv1 cells described in *B* were maintained in growth media that contained 5% charcoal-stripped FBS supplemented with enzalutamide (Enza; 5 μM) or R1881 (1 nM). After 24 h, RNAs were collected and analyzed by qRT-PCR for transcripts of representative AR target genes that include NKX3.1, FKBP5, and SREBF1. (*D*) AR-V7 was reexpressed in JMJD1A-knockdown Rv1 cells via lentiviral transduction (shJMJD1A+AR-V7). Cell lysates were analyzed by Western blotting with antibodies against AR-V7 or JMJD1A. (*E*) Rv1 cells (pLKO.1, shJMJD1A, or shJMJD1A+AR-V7) were treated and analyzed by qRT-PCR as described in *C*. In *C* and *E*, the comparison with statistical significance is indicated with an asterisk (**$P < 0.01$, *$P < 0.05$; ANOVA).

AR-V7 using shRNA that targeted the AR-V7 3′-UTR. Western blot and qRT-PCR analysis showed that levels of AR-FL or AR-V7 in Rv1 cells were efficiently and specifically knocked down by the respective shRNAs (Fig. 2*B* and Fig. S2*A*). As another control, AR-FL or AR-V7 shRNAs showed no effect on the mRNA level of AR-V1, another form of AR variant (Fig. S2*A*). Of note, knockdown of AR-V7 significantly reduced the level of AR-Vs (Fig. 2*B*), indicating that AR-V7 is the major form of AR-Vs in Rv1 cells. We next performed qRT-PCR analysis on a panel of well-characterized AR targets that include KLK3, NKX3.1, SLC45A3, FKBP5, NDRG1, SREBF1, STEAP1, and STEAP2. In Rv1 cells, the sample AR targets can be categorized into three groups (Fig. 2*C* and Fig. S2*B*): (*i*) AR targets, such as NKX3.1, KLK3, SLC45A3, or STEAP2, depend on AR-FL in normal androgen conditions but become dependent on AR-V7 under androgen-deprived conditions; (*ii*) AR targets, such as FKBP5, NDRG1, or STEAP1, depend on both AR-FL and AR-V7 in normal androgen conditions but depend mainly on AR-V7 under androgen-deprived conditions; and (*iii*) AR targets, such as SREBF1, are only dependent on AR-V7 under either normal or androgen-deprived conditions. Therefore, we chose NKX3.1, FKBP5, and SREBF1 as representative examples of each of the three AR target groups regulated by AR-FL and/or AR-V7 in Rv1 cells. We restored AR-V7 expression in JMJD1A-knockdown Rv1 cells to the control levels (Fig. 2*D*) and examined expression of representative AR targets by qRT-PCR (Fig. 2*E*). Under androgen deprivation conditions, reexpression of AR-V7 in JMJD1A-knockdown Rv1 cells rescued expression of NKX3.1, FKBP5, and SREBF1 (Fig. 2*E*), consistent with the dependency of these AR targets on AR-V7 in the absence of androgen (Fig. 2*C*). In contrast, under normal androgen conditions, reexpression of AR-V7 in the JMJD1A-knockdown Rv1 cells fully rescued SREBF1 expression, partly rescued FKBP5 expression, but had no effect on NKX3.1 expression (Fig. 2*E*). These data are consistent with the dependency of SREBF1 on AR-V7, partial dependency of FKBP5 on AR-V7,

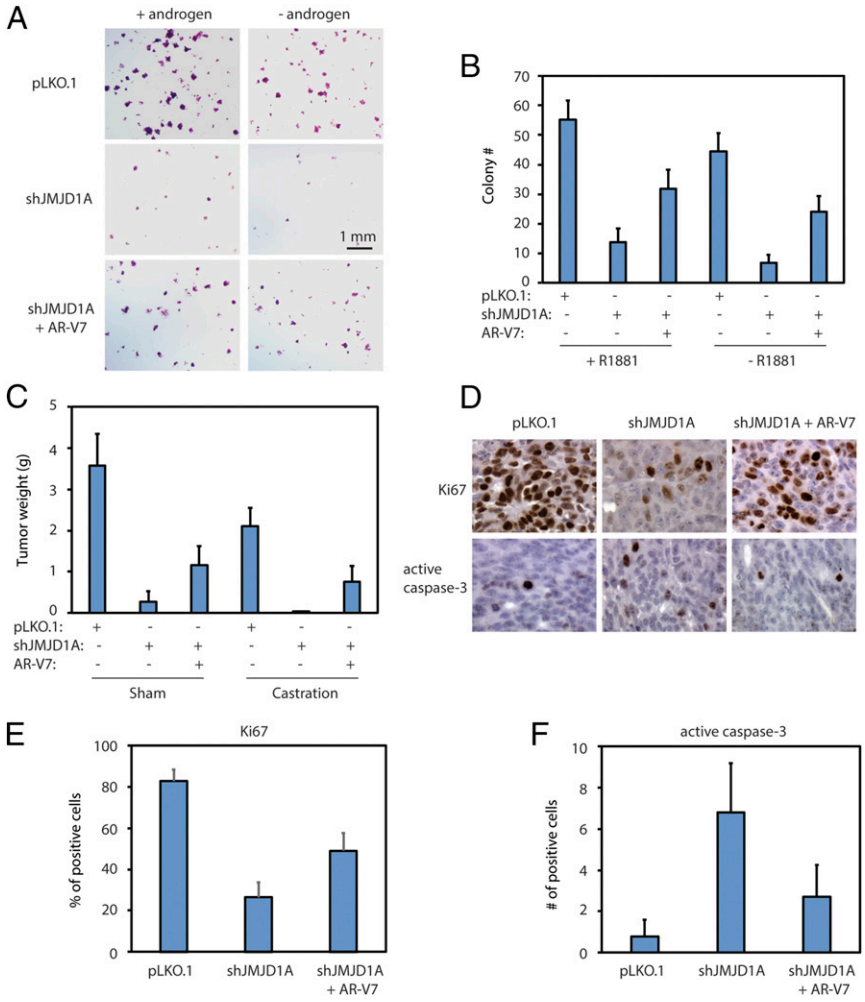

Fig. 3. (*A* and *B*) Rv1 cells (pLKO.1, shJMJD1A, or shJMJD1A+AR-V7) were seeded at low density and maintained for 3 wk in 5% charcoal-stripped FBS media with or without 1 nM R1881 supplement. Colony number (>100 μm in diameter) was scored after 3 wk. Representative images of colonies are shown in *A*, and the colony number per high-power field is shown in *B*. +R1881, $P < 0.001$ for any pairwise comparison (ANOVA); −R1881, $P < 0.001$ for any pairwise comparison (ANOVA). (*C*) Rv1 cells (pLKO.1, shJMJD1A, or shJMJD1A+AR-V7) were injected s.c. into immune-deficient NSG mice ($n = 20$ per group). After 1 wk, half of the mice in each group were castrated, while the other half were sham-castrated. The xenograft tumors were collected, and tumor weight was measured 2 wk later. For sham conditions, $P < 0.001$ for any pairwise comparison (ANOVA); for castration conditions, $P < 0.001$ for any pairwise comparison (ANOVA). (*D*) Example staining of Ki67 (*Upper*) and active caspase-3 (*Lower*) on tumor sections derived from the indicated Rv1 cells. The staining was developed by DAB (brown) and counterstained by hematoxylin (blue). The image width is 0.5 mm. (*E*) Percentage of Ki67-positive cells per field on the staining described in *D*. $P < 0.01$ for shJMJD1A vs. shJMJD1A+AR-V7 (ANOVA); $P < 0.001$ for other pairwise comparisons (ANOVA). (*F*) Number of positive cells for active caspase-3 per field on staining described in *D*. $P < 0.001$ for pLKO.1 vs. shJMJD1A (ANOVA); $P < 0.01$ for other pairwise comparisons (ANOVA).

and dependency of NKX3.1 on AR-FL in the presence of androgens (Fig. 2*C*). Taken together, the above results demonstrate that JMJD1A-dependent expression of AR-V7 in Rv1 cells promotes expression of AR targets that rely on AR-V7.

AR-V7 Is a Downstream Effector of JMJD1A in Rv1 Cells. To assess the effect of AR-V7 on JMJD1A-dependent cell growth, we evaluated colony formation by JMJD1A-knockdown Rv1 cells upon restoring the expression of AR-V7 in these cells (shJMJD1A+ AR-V7), as described in Fig. 2*D*. The Rv1 cells were allowed to form colonies in the presence or absence of androgen. Compared with the pLKO.1 control, JMJD1A-knockdown Rv1 cells showed about a fivefold reduction in colony formation (Fig. 3 *A* and *B*). Reexpression of AR-V7 in JMJD1A-knockdown Rv1 cells partially increased their ability to form colonies (Fig. 3 *A* and *B*). Comparable results were seen for Rv1 cells grown in the presence or absence of androgen, although the presence of androgen slightly increased colony formation (Fig. 3 *A* and *B*).

To further test the role of AR-V7 in JMJD1A-dependent tumor growth in vivo, we used a xenograft prostate tumor model in which Rv1 cells were injected s.c. into immune-deficient NSG mice. Compared with control cells, JMJD1A-knockdown Rv1 cells showed an ∼13-fold reduction in tumor weights in the control mice, with no tumor formation in castrated mice (Fig. 3*C*). Reexpression of AR-V7 in JMJD1A-knockdown Rv1 cells partly rescued xenograft tumor formation in both control and castrated mice (Fig. 3*C*). We next performed immunohistochemistry staining for the proliferation marker Ki67 and the apoptosis marker active caspase-3 on xenograft tumor sections. JMJD1A knockdown reduced the percentage of Ki67-positive cells, concomitant with an increased number of cells positive for active caspase-3 (Fig. 3 *D*–*F*). These results suggest that JMJD1A knockdown inhibits proliferation and promotes apoptosis in xenograft prostate tumors. In contrast, the patterns of Ki67 and active caspase-3 staining detected in JMJD1A-knockdown tumors were partially reversed after AR-V7 reexpression (Fig. 3 *D*–*F*). Overall, these findings confirmed that AR-V7 could function as a downstream effector of JMJD1A to drive the growth and survival of prostate cancer cells under normal or androgen-deprived conditions.

JMJD1A Promotes Splicing of AR-V7 Through HNRNPF. In contrast to the splicing of AR-FL mRNA, which uses the 3′ splice site in front of exon 4, the splicing of AR-V7 mRNA uses an alternative 3′ splice site in front of the cryptic exon 3b (Fig. 4*A*), which results in translation of an AR protein with a truncated C terminus

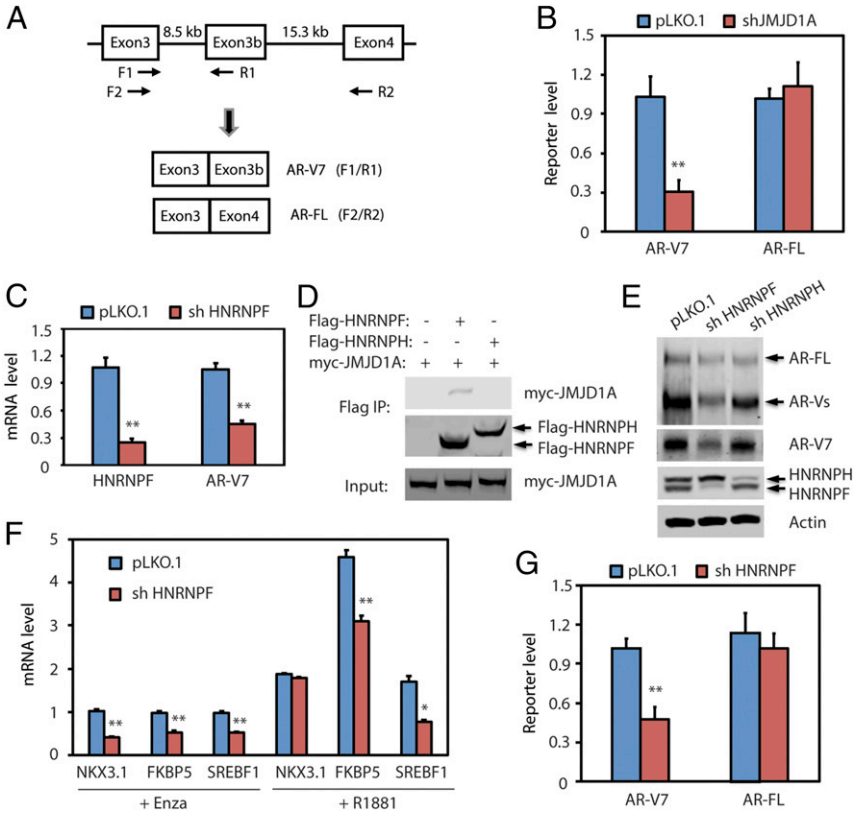

Fig. 4. (*A*) Diagram of the AR minigene reporter. Exons, introns, and PCR primers used to detect exon splicing are indicated in the diagram. Splicing between exons 3 and 3b reflects formation of AR-V7 mRNA, which can be detected by the F1/R1 primer pair. Splicing between exons 3 and 4 reflects formation of AR-FL mRNA, which can be detected by the F2/R2 primer pair. (*B*) PC3 cells (pLKO.1 or shJMJD1A) were transfected with the AR minigene reporter. After 72 h, RNAs were isolated and analyzed by qRT-PCR using the F1/R1 or F2/R2 primer pair, which reflects the levels of AR-V7 or AR-FL, respectively. (*C*) Rv1 cells were transduced with pLKO.1 control or HNRNPF shRNA. After 48 h, RNAs were isolated and analyzed by qRT-PCR for HNRNPF or AR-V7. (*D*) Flag-tagged HNRNPF or HNRNPH was cotransfected with myc-JMJD1A in 293T cells. Cell lysates were subjected to immunoprecipitation (IP) with anti-Flag M2 beads. Bound proteins were analyzed by Western blotting with myc or Flag antibodies. (*E*) Rv1 cells were transduced with pLKO.1 control, HNRNPF, or HNRNPH shRNAs. After 48 h, cell lysates were analyzed by Western blotting with AR antibody (N-20, *Top*) or other indicated antibodies. (*F*) Rv1 cells (pLKO.1 or HNRNPF-knockdown) were maintained in growth media containing 5% charcoal-stripped FBS supplemented with either enzalutamide (Enza; 5 μM) or R1881 (1 nM) for 24 h. RNAs were isolated and analyzed by qRT-PCR for transcripts of representative AR target genes. (*G*) PC3 cells (pLKO.1 or HNRNPF-knockdown) were transfected with the AR minigene reporter. After 72 h, RNAs were isolated and analyzed by qRT-PCR to detect reporter levels of AR-V7 or AR-FL, respectively. In *B*, *C*, *F*, and *G*, the comparison with statistical significance is indicated with an asterisk (**$P < 0.01$, *$P < 0.05$; *t* test).

(4, 5). To determine if JMJD1A could affect AR-V7 mRNA splicing, we used an AR-V7 minigene reporter plasmid, in which exon 3b and its flanking ∼400-bp nucleotide sequence were inserted between exons 3 and 4 of the human AR gene (23). The plasmid was transfected into AR-negative PC3 prostate cancer cells (pLKO.1 control or JMJD1A knockdown), followed by qRT-PCR analysis of the spliced product reflecting AR-V7 (splicing between exon 3 and 3b) or AR-FL (splicing between exon 3 and 4) (Fig. 4*A*). We found that JMJD1A knockdown reduced the splicing of AR-V7 but had no apparent effect on the splicing of AR-FL (Fig. 4*B*). These results indicate that JMJD1A promotes splicing of AR-V7 mRNA.

We next addressed the mechanism by which JMJD1A promotes the splicing of AR-V7. We first hypothesized that JMJD1A may promote the expression of factors that play a role in AR-V7 splicing. We reexamined our previous profiling array data (GSE70498) on the JMJD1A-knockdown Rv1 cells (15) and searched the known RNA splicing regulators whose expression was regulated by JMJD1A. We chose SYF2, SRSF7, PHF5A, RBFOX2, SREK1, RAVER2, and ESRP1 for further analysis because they were among the highly down-regulated genes in the JMJD1A-knockdown cells and are known to regulate mRNA splicing. However, individual knockdown of these splicing regulators in Rv1 cells showed no effect on AR-V7 mRNA levels (Fig. S3*A*). This excluded the involvement of these seven splicing regulators examined, although we could not exclude the possible involvement of other JMJD1A-dependent genes in splicing events that generate AR-V7. We next tested a second hypothesis that JMJD1A may interact with a splicing regulator to promote AR-V7 splicing. Mass spectrometry analysis of proteins that coprecipitated with Flag-JMJD1A in Rv1 cells revealed nine candidate proteins (Table S1), among which HNRNPF, PTBP1, and YBX1 were known to regulate mRNA splicing. We found that knockdown of HNRNPF, but not PTBP1 or YBX1, reduced the levels of AR-V7 mRNA in Rv1 cells (Fig. 4*C* and Fig. S3*B*). Consistent with the MS results, we found that myc-JMJD1A coprecipitated with Flag-HNRNPF, but not Flag-HNRNPH, which is a close relative of HNRNPF (Fig. 4*D*). Knockdown of HNRNPF in Rv1 cells reduced AR-V7 protein levels but had little effect on those of AR-FL (Fig. 4*E*). In contrast, knockdown of HNRNPH had little effect on either AR-V7 or AR-FL (Fig. 4*E*). The qRT-PCR analysis revealed that the effects of HNRNPF knockdown with respect to the expression of sample AR targets (Fig. 4*F*) resembled those of AR-V7 knockdown (Fig. 2*C*). Similarly, the AR-V7 minigene reporter assay demonstrated that HNRNPF knockdown reduced splicing of AR-V7, but not AR-FL (Fig. 4*G*). We also examined the staining of HNRNPF on 36 specimens of human prostate cancer tissue. HNRNPF displayed strong nuclear staining in all of the samples (Fig. S4), indicating that HNRNPF is highly expressed in prostate cancer.

HNRNPF binds to the G-tract sequences that contain at least three consecutive G's (G-triplet) on pre-mRNA to regulate splicing (24). Within a 200-bp region around the 3′ splice site of exon 3b, there are five G-tracts in the downstream exon 3b sequence (Fig. 5*A*) but none in the upstream intron sequence. To determine if AR-V7 splicing required any of the five G-tracts, we mutated each G-tract sequence in the AR-V7 minigene reporter. Mutation of the first G-tract adjacent to the 3′ splice site reduced AR-V7 splicing, whereas mutation of the other G-tracts had no effect (Fig. 5*B*). To determine if HNRNPF could bind to the identified G-tract, we synthesized an RNA oligo representing either a wild-type (WT) or mutant G-tract sequence for RNA pull-down experiments. We found that purified HNRNPF could be pulled down by the WT oligo (Fig. 5*C*, lane 3), whereas pull-down

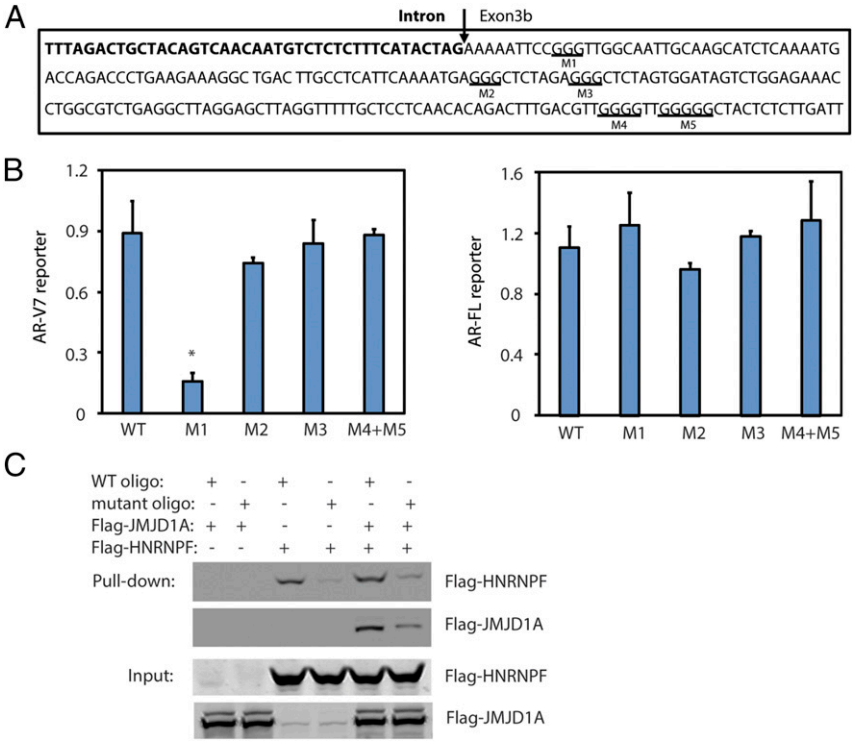

Fig. 5. (*A*) Partial sequence of intron 3 (bold) and exon 3b from the AR gene. The first three G-tracts (underlined) were individually mutated in the AR minigene reporter (M1 to M3), while the last two G-tracts were simultaneously mutated (M4 + M5). (*B*) PC3 cells were transfected with the AR minigene reporter (WT or G-tract mutants). After 72 h, RNAs were isolated and analyzed by qRT-PCR to detect reporter levels of AR-V7 or AR-FL, respectively. (*C*) Purified Flag-HNRNPF and/or Flag-JMJD1A was incubated with RNA oligo-conjugated beads (WT or G-tract mutant). The beads were washed, and bound proteins were analyzed by Western blotting using anti-Flag antibodies.

of HNRNPF by the mutant oligo was reduced (Fig. 5*C*, lane 4). These results indicate that HNRNPF binds to the G-tract sequence within the RNA oligo. Purified JMJD1A alone was not pulled down by the WT oligo (Fig. 5*C*, lane 1); however, pull-down of JMJD1A by the WT RNA oligo was detected after the addition of HNRNPF (Fig. 5*C*, lane 5). Similarly, the mutant RNA oligo showed a reduced capability to pull down JMJD1A in the presence of HNRNPF (Fig. 5*C*, lane 6). These results indicate that JMJD1A may bind to the G-tract sequence through HNRNPF. Interestingly, addition of JMJD1A slightly increased the pull-down of HNRNPF by the WT oligo (Fig. 5*C*, lane 3 vs. lane 5), suggesting that JMJD1A–HNRNPF interaction may enhance the binding of HNRNPF to the G-tract sequence. Taken together, these data reveal that HNRNPF, an mRNA splicing factor that interacts with JMJD1A, plays a role in AR-V7 splicing.

JMJD1A Promotes the Recruitment of HNRNPF and Spliceosome Component to Exon 3b of AR Pre-mRNA. The RNA pull-down experiments indicate that JMJD1A and HNRNPF can bind to the G-tract sequence in vitro. To determine if JMJD1A and HNRNPF could also bind to the same site in the AR pre-mRNA, we performed RNA immunoprecipitation (RIP) assays. We immunoprecipitated JMJD1A or HNRNPF from the lysates of Rv1 cells, and the bound RNAs were isolated for qRT-PCR analysis using two sets of primers. The first set of primers targeted the P1 region (i.e., the 3′ splice site of exon 3b) of AR pre-mRNA, and the second set of primers targeted the P2 region (i.e., the 3′ splice site of exon 4) (Fig. 6*A*). The RIP assays showed that HNRNPF and JMJD1A were both enriched in the P1, but not the P2, region of AR pre-mRNA (Fig. 6 *B* and *C*), which is consistent with the function of JMJD1A and HNRNPF to splice AR-V7, but not AR-FL. HNRNPF knockdown had no effect on the levels of JMJD1A (Fig. S5*A*) but reduced JMJD1A enrichment at the P1 region (Fig. 6*C*). Again, these results are consistent with the result of RNA pull-down experiments showing that JMJD1A likely binds to this region through an interaction with HNRNPF. JMJD1A knockdown also had no effect on HNRNPF levels (Fig. S5*B*). However, the RIP assays showed that JMJD1A knockdown strongly reduced HNRNPF enrichment at the P1 region (Fig. 6*B*), suggesting that JMJD1A

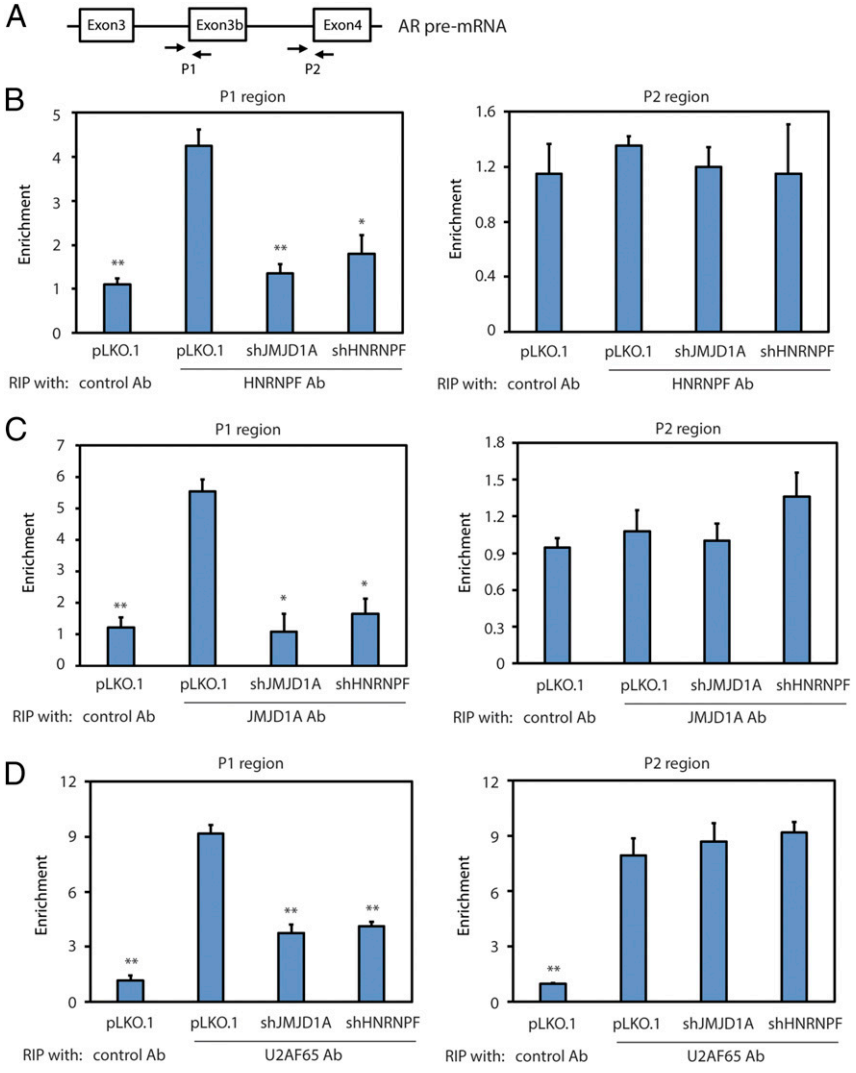

Fig. 6. (*A*) Diagram showing primers used to amplify the P1 or P2 region of AR pre-mRNA in the RIP assays. (*B*) Rv1 cells (control, JMJD1A-knockdown, or HNRNPF-knockdown) were subjected to RIP assays using HNRNPF antibodies (Ab). Precipitated RNAs were isolated and analyzed by qRT-PCR with primers that amplified the P1 or P2 region. Data were calculated as the percentage of input and plotted as fold change over control (Ab). (*C*) Rv1 cells (control, JMJD1A-knockdown, or HNRNPF-knockdown) were subjected to RIP assays with JMJD1A Ab. The results were analyzed as described in *B*. (*D*) Rv1 cells (control, JMJD1A-knockdown, or HNRNPF-knockdown) were subjected to RIP assays using U2AF65 Ab. The results were analyzed as described in *B*.

plays a key role in the binding of HNRNPF to this region of AR pre-mRNA.

We next tested whether JMJD1A and HNRNPF could affect the recruitment of spliceosome components to the 3′ splice site in front of exon 3b. We performed the RIP assay using antibodies to U2AF65, which is one of the spliceosome components associated near the 3′ splice site. We found that knockdown of either JMJD1A or HNRNPF reduced U2AF65 enrichment at the P1 region but had no effect on its enrichment at the P2 region (Fig. 6*D*). As a control, knockdown of HNRNPF or JMJD1A showed no effect on U2AF65 levels (Fig. S5 *A* and *B*). To determine if HNRNPF and JMJD1A can directly recruit U2AF65, we purified U2AF65 for the in vitro RNA pull-down experiments as described in the legend for Fig. 5*C*. As expected, the RNA oligo, which lacks the U2AF65 binding site, failed to directly pull down U2AF65 (Fig. S5*C*, lane 1). In contrast, addition of HNRNPF led to the pull-down of U2AF65 by WT, but not the G-tract, mutant oligo (Fig. S5*C*, lane 3 vs. lane 4). These results suggest that U2AF65 may associate with the RNA oligo through HNRNPF. Addition of JMJD1A further increased the pull-down of both HNRNPF and U2AF65 by the RNA oligo (Fig. S5*C*, lane 3 vs. lane 5). Taken together, the results of RIP and RNA pull-down experiments indicate that JMJD1A–HNRNPF interaction promotes the recruitment of a spliceosome component to the 3′ splice site region of exon 3b on AR pre-mRNA.

JMJD1A Recruits HNRNPF to Exon 3b of AR Genomic DNA. Some splicing factors can associate with chromatin to facilitate the cotranscriptional mRNA splicing (25, 26). Because JMJD1A is a histone demethylase that can associate with chromatin, we determined to test if JMJD1A and HNRNPF associate with the chromatin region of the AR gene. We performed chromatin immunoprecipitation (ChIP) assays on the chromatin fragments prepared from Rv1 cells using antibodies of JMJD1A, HNRNPF, or H3K9me2. The precipitated DNA fragments were analyzed by qPCR using the same set of primers that were used for the RIP assay (Fig. 7*A*). The ChIP assays showed that HNRNPF and JMJD1A were enriched at the P1, but not the P2, region (Fig. 7 *B* and *C*), indicating their chromatin association near the 3′

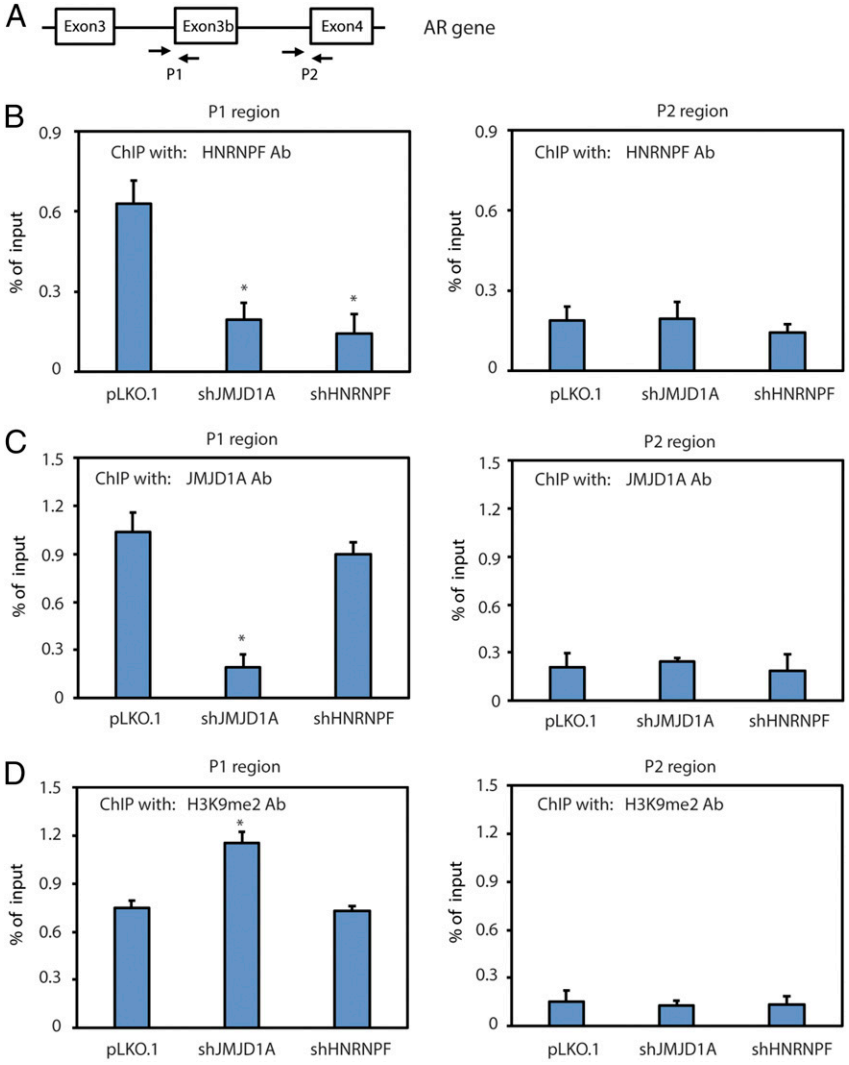

Fig. 7. (*A*) Diagram showing primers used to amplify the P1 or P2 region of the AR gene in the ChIP assays. (*B*) Rv1 cells (control, JMJD1A-knockdown, or HNRNPF-knockdown) were subjected to ChIP assays using HNRNPF antibodies (Ab). Precipitated chromatin fragments were isolated and analyzed by qPCR with primers that amplified the P1 or P2 region. Data were calculated as the percentage of input. (*C*) Rv1 cells (control, JMJD1A-knockdown, or HNRNPF-knockdown) were subjected to ChIP assays using JMJD1A Ab. The results were analyzed as described in *B*. (*D*) Rv1 cells (control, JMJD1A-knockdown, or HNRNPF-knockdown) were subjected to ChIP assays using H3K9me2 Ab. The results were analyzed as described in *B*.

splice site of exon 3b. JMJD1A knockdown reduced the enrichment of HNRNPF at the P1 region similar to that seen upon HNRNPF knockdown (Fig. 7*B*), indicating that JMJD1A may mediate the binding of HNRNPF with this chromatin region. In contrast, HNRNPF knockdown showed no effect on the enrichment of JMJD1A at the P1 region (Fig. 7*C*), indicating that HNRNPF does not affect the chromatin binding of JMJD1A. The ChIP assays also revealed the enrichment of H3K9me2 marks at the P1, but not the P2, region, and the increased level of H3K9me2 at the P1 region upon JMJD1A knockdown (Fig. 7*D*). Together, these results indicate that H3K9me2 may recruit JMJD1A, and thus HNRNPF, to exon 3b of AR genomic DNA.

Discussion

Regulation of AR-V7 alternative splicing is of critical importance to the expression of AR-V7 and CRPC progression. AR-V7 alternative splicing couples with AR gene transcription and is facilitated by AR gene amplification/rearrangement (23, 27). However, the mechanisms that control this process remain poorly understood. Here, we have identified JMJD1A as a key regulator for alternative splicing of AR pre-mRNA to generate AR-V7.

JMJD1A functions as a key coactivator of AR and regulates the AR transcriptional program in prostate cancer cells through H3K9 demethylation (13, 15, 16). Our current study reveals a role for JMJD1A in the splicing and generation of AR-V7 in prostate cancer cells. Thus, JMJD1A may use two mechanisms to regulate AR transcriptional activity. JMJD1A possesses an LXXLL motif, which is present in some coactivators and known to interact with the LBD of nuclear receptors (28). As AR-V7 lacks an LBD, JMJD1A may not function as a coactivator for AR-V7. Consistent with this, our results show that JMJD1A interacts with AR-FL, but not AR-V7. Moreover, restoration of AR-V7 in the JMJD1A-knockdown cells increased the expression of representative AR targets that depend on AR-V7, but not AR-FL. Thus, JMJD1A-dependent coactivation of AR-FL and formation of AR-V7 may represent two distinct mechanisms for JMJD1A in the regulation of AR activity.

The splicing factor, HNRNPF, can enhance or inhibit alternative splicing in a context-dependent manner (17–21). Our data revealed that JMJD1A promoted the recruitment of HNRNPF to exon 3b of AR pre-mRNA for AR-V7 splicing. Our in vitro RNA pull-down experiments showed that purified JMJD1A slightly enhanced the association of purified HNRNPF with a 40-bp RNA oligo derived from exon 3b. In contrast to the moderate effect seen in the in vitro RNA pull-down experiments, our RIP assay showed that JMJD1A knockdown drastically reduced HNRNPF binding with the exon 3b region of AR pre-mRNA. The discrepancy may be due to the fact that the short RNA oligo lacks the secondary structure seen in the full pre-mRNA, which is known to affect binding of splicing factors (29). Importantly, our ChIP assay showed that JMJD1A recruits HNRNPF to the chromatin region of AR exon 3b that displays H3K9 methylation marks. This chromatin localization of the JMJD1A–HNRNPF complex may facilitate the binding of JMJD1A and HNRNPF to exon 3b of transcribing AR pre-mRNA before the formation of RNA secondary structures. Thus, the chromatin localization of the JMJD1A–HNRNPF complex may represent an additional mechanism for JMJD1A-dependent recruitment of HNRNPF to exon 3b of AR pre-mRNA.

HNRNPF and HNRNPH are homologous proteins, but they may also differentially regulate RNA alternative splicing (17, 18). The interaction of JMJD1A with HNRNPF, but not with HNRNPH, may underlie the specificity of HNRNPF in the AR-V7 splicing. HNRNPF/H binds to the G-tract sequence (24), while the adjacent nucleotide sequence of the G-tract may modulate the binding and splicing activity of HNRNPF/H (30, 31). Although there are multiple G-tracts in exon 3b, we found that only the first G-tract, 10-bp downstream of the 3′ splice site, functioned in AR-V7 generation, as revealed by the AR minigene splicing assay. HNRNPF/H can interact with spliceosome components or other splicing factors in the regulation of mRNA splicing (21, 32–34). U2AF65 is one of the spliceosome components that associate with the sequence near the 3′ splice site. We found that HNRNPF promoted recruitment of U2AF65 to the 3′ splice site around exon 3b of AR pre-mRNA. Thus, the close proximity of the HNRNPF binding site to the 3′ splice site of exon 3b may facilitate spliceosome component(s) recruitment for recognition and inclusion of exon 3b to enable AR-V7 splicing.

JMJD1A can act to demethylate H3K9, as well as nonhistone proteins (13, 35). It was recently reported that JMJD6, an arginine demethylase and lysine hydroxylase, could regulate the alternative splicing by hydroxylating U2AF65 (36). It remains to be determined whether the demethylase activity of JMJD1A or JMJD6 is involved in the RNA alternative splicing. The splicing factor HNRNPA1 was reported to increase the expression of AR-V7 in prostate cancer cells, although it was unclear if HNRNPA1 promoted the splicing of AR-V7 (37). Interestingly, HNRNPA1 and HNRNPF were reported to cooperate in the splicing of some pre-mRNAs (33, 34). It will be interesting to determine whether the JMJD1A–HNRNPF complex interplays with HNRNPA1 for the AR-V7 splicing.

We have elucidated a mechanism for JMJD1A in the splicing of AR-V7 in prostate cancer cell lines. This mechanism may also function in some human prostate cancers. We found that the staining of JMJD1A and AR-V7 paralleled one another in a subset of human prostate cancer tissue. In contrast, the staining of HNRNPF was highly expressed in all of the human prostate cancer tissues examined. Thus, the level of JMJD1A or factors that regulate the JMJD1A–HNRNPF interaction may control the alternative splicing of AR-V7 in prostate cancer.

Increased levels of AR-FL and AR-V7 are not uncommon events during CRPC progression (1, 7, 38). Current therapeutic strategies are aimed at targeting against AR-FL but are unlikely to have significant effects in prostate cancers that express AR-V7. Our findings that JMJD1A regulates the activity of AR-FL and generation of AR-V7 suggest that future development of specific JMJD1A inhibitors may be a promising strategy to target advanced stages of prostate cancer.

Materials and Methods

Antibodies and Reagents. Antibodies were acquired from the following companies: AR (sc-816), myc (sc-789 or sc-40), HNRNPF/H (sc-32310), and U2AF65 (sc-53942) were from Santa Cruz Biotechnology; JMJD1A (A301-539A or 538A) was from Bethyl Laboratories; JMJD1A (12835-1-AP) was from Proteintech; AR-V7 (ab198394), HNRNPF (ab50982), and Ki67 (ab8191) were from Abcam; active caspase-3 (9661) was from Cell Signaling; H3K9me2 (07-441) was from EMD Millipore; and Flag (F7425) and actin (A5441) were from Sigma–Aldrich. All were used according to the manufacturers' recommendations.

Cell Lines. Rv1 cells were kindly provided by James Jacobberger, Case Western Reserve University, Cleveland. C4-2 cells were provided by Leland Chung, Cedars-Sinai Medical Center, Los Angeles. Rv1 and C4-2 cells were maintained in RPMI 1640 media supplemented with 10% FBS and antibiotics. LN95 cells were provided by Alan Meeker, Johns Hopkins University, Baltimore, and maintained in RPMI 1640 media with 5% charcoal-stripped FBS and antibiotics. VCaP cells were purchased from the American Type Culture Collection and maintained in DMEM media supplemented with 10% FBS and antibiotics. All prostate cancer cells were regularly tested to ensure that they remained mycoplasma-free.

Animal Studies. NSG mice were purchased from and housed in the animal facility at the University of Maryland School of Medicine. All experiments were approved by the Institutional Animal Care and Use Committee (IACUC no. 0613011) and conducted following the institute's animal policies in accordance with NIH guidelines.

Prostate Tumor Samples. A total of 40 prostate cancer specimens with Gleason scores 3–5 were obtained from the Vancouver Prostate Tissue Bank at the University of British Columbia (Clinical Research Ethics Board no. H09-01628). All specimens were obtained from radical prostatectomy samples with informed consent. H&E slides were reviewed, and desired areas were marked. The TMA was manually constructed (Beecher Instruments) and used for immunohistochemistry staining.

Statistical Analysis. The in vitro experiments were repeated at least three times. Data are presented as the mean ± SD. The Student's *t* test (two-tailed) was used to compare the difference between two groups of datasets with similar variance. The ANOVA test was used to compare the difference between more than two groups of datasets. The Mann–Whitney *U* test was used to assess the relationship between JMJD1A and AR-V7 staining. *P* values less than 0.05 were considered statistically significant. Compared with controls, the statistical difference is labeled as * ($P < 0.05$), ** ($P < 0.01$), or *** ($P < 0.001$).

Additional methods are presented in *SI Materials and Methods*.

ACKNOWLEDGMENTS. This study is supported by National Cancer Institute Grant R01CA207118 and V Scholar Award V2016-026 (to J.Q.). Part of A.H.'s time was supported by a Merit Review Award (I01 BX000545), Medical Research Service, Department of Veterans Affairs.

1. Robinson D, et al. (2015) Integrative clinical genomics of advanced prostate cancer. *Cell* 162:454.
2. Watson PA, Arora VK, Sawyers CL (2015) Emerging mechanisms of resistance to androgen receptor inhibitors in prostate cancer. *Nat Rev Cancer* 15:701–711.
3. Sun S, et al. (2010) Castration resistance in human prostate cancer is conferred by a frequently occurring androgen receptor splice variant. *J Clin Invest* 120:2715–2730.
4. Guo Z, et al. (2009) A novel androgen receptor splice variant is up-regulated during prostate cancer progression and promotes androgen depletion-resistant growth. *Cancer Res* 69:2305–2313.
5. Hu R, et al. (2009) Ligand-independent androgen receptor variants derived from splicing of cryptic exons signify hormone-refractory prostate cancer. *Cancer Res* 69: 16–22.
6. Antonarakis ES, et al. (2014) AR-V7 and resistance to enzalutamide and abiraterone in prostate cancer. *N Engl J Med* 371:1028–1038.
7. Hörnberg E, et al. (2011) Expression of androgen receptor splice variants in prostate cancer bone metastases is associated with castration-resistance and short survival. *PLoS One* 6:e19059.
8. Chan SC, et al. (2015) Targeting chromatin binding regulation of constitutively active AR variants to overcome prostate cancer resistance to endocrine-based therapies. *Nucleic Acids Res* 43:5880–5897.
9. Watson PA, et al. (2010) Constitutively active androgen receptor splice variants expressed in castration-resistant prostate cancer require full-length androgen receptor. *Proc Natl Acad Sci USA* 107:16759–16765.
10. Xu D, et al. (2015) Androgen receptor splice variants dimerize to transactivate target genes. *Cancer Res* 75:3663–3671.
11. Hu R, et al. (2012) Distinct transcriptional programs mediated by the ligand-dependent full-length androgen receptor and its splice variants in castration-resistant prostate cancer. *Cancer Res* 72:3457–3462.
12. Li Y, et al. (2013) Androgen receptor splice variants mediate enzalutamide resistance in castration-resistant prostate cancer cell lines. *Cancer Res* 73:483–489.
13. Yamane K, et al. (2006) JHDM2A, a JmjC-containing H3K9 demethylase, facilitates transcription activation by androgen receptor. *Cell* 125:483–495.
14. Tateishi K, Okada Y, Kallin EM, Zhang Y (2009) Role of Jhdm2a in regulating metabolic gene expression and obesity resistance. *Nature* 458:757–761.
15. Fan L, et al. (2016) Regulation of c-Myc expression by the histone demethylase JMJD1A is essential for prostate cancer cell growth and survival. *Oncogene* 35: 2441–2452.
16. Wilson S, Fan L, Sahgal N, Qi J, Filipp FV (2017) The histone demethylase KDM3A regulates the transcriptional program of the androgen receptor in prostate cancer cells. *Oncotarget* 8:30328–30343.
17. Wang E, Cambi F (2009) Heterogeneous nuclear ribonucleoproteins H and F regulate the proteolipid protein/DM20 ratio by recruiting U1 small nuclear ribonucleoprotein through a complex array of G runs. *J Biol Chem* 284:11194–11204.
18. Min H, Chan RC, Black DL (1995) The generally expressed hnRNP F is involved in a neural-specific pre-mRNA splicing event. *Genes Dev* 9:2659–2671.
19. Garneau D, Revil T, Fisette JF, Chabot B (2005) Heterogeneous nuclear ribonucleoprotein F/H proteins modulate the alternative splicing of the apoptotic mediator Bcl-x. *J Biol Chem* 280:22641–22650.
20. Lefave CV, et al. (2011) Splicing factor hnRNPH drives an oncogenic splicing switch in gliomas. *EMBO J* 30:4084–4097.
21. Crawford JB, Patton JG (2006) Activation of alpha-tropomyosin exon 2 is regulated by the SR protein 9G8 and heterogeneous nuclear ribonucleoproteins H and F. *Mol Cell Biol* 26:8791–8802.
22. Cai C, et al. (2011) Androgen receptor gene expression in prostate cancer is directly suppressed by the androgen receptor through recruitment of lysine-specific demethylase 1. *Cancer Cell* 20:457–471.
23. Liu LL, et al. (2014) Mechanisms of the androgen receptor splicing in prostate cancer cells. *Oncogene* 33:3140–3150.
24. Dominguez C, Allain FH (2006) NMR structure of the three quasi RNA recognition motifs (qRRMs) of human hnRNP F and interaction studies with Bcl-x G-tract RNA: A novel mode of RNA recognition. *Nucleic Acids Res* 34:3634–3645.
25. Luco RF, et al. (2010) Regulation of alternative splicing by histone modifications. *Science* 327:996–1000.
26. Piacentini L, et al. (2009) Heterochromatin protein 1 (HP1a) positively regulates euchromatic gene expression through RNA transcript association and interaction with hnRNPs in Drosophila. *PLoS Genet* 5:e1000670.
27. Li Y, et al. (2011) Intragenic rearrangement and altered RNA splicing of the androgen receptor in a cell-based model of prostate cancer progression. *Cancer Res* 71: 2108–2117.
28. Chang Cy, et al. (1999) Dissection of the LXXLL nuclear receptor-coactivator interaction motif using combinatorial peptide libraries: Discovery of peptide antagonists of estrogen receptors alpha and beta. *Mol Cell Biol* 19:8226–8239.
29. Buratti E, Baralle FE (2004) Influence of RNA secondary structure on the pre-mRNA splicing process. *Mol Cell Biol* 24:10505–10514.
30. Wang Y, Ma M, Xiao X, Wang Z (2012) Intronic splicing enhancers, cognate splicing factors and context-dependent regulation rules. *Nat Struct Mol Biol* 19:1044–1052.
31. Jablonski JA, Buratti E, Stuani C, Caputi M (2008) The secondary structure of the human immunodeficiency virus type 1 transcript modulates viral splicing and infectivity. *J Virol* 82:8038–8050.
32. Jacquenet S, et al. (2001) A second exon splicing silencer within human immunodeficiency virus type 1 tat exon 2 represses splicing of Tat mRNA and binds protein hnRNP H. *J Biol Chem* 276:40464–40475.
33. Martinez-Contreras R, et al. (2006) Intronic binding sites for hnRNP A/B and hnRNP F/H proteins stimulate pre-mRNA splicing. *PLoS Biol* 4:e21.
34. Han K, Yeo G, An P, Burge CB, Grabowski PJ (2005) A combinatorial code for splicing silencing: UAGG and GGGG motifs. *PLoS Biol* 3:e158.
35. Ramadoss S, Guo G, Wang CY (2017) Lysine demethylase KDM3A regulates breast cancer cell invasion and apoptosis by targeting histone and the non-histone protein p53. *Oncogene* 36:47–59.
36. Yi J, et al. (2017) JMJD6 and U2AF65 co-regulate alternative splicing in both JMJD6 enzymatic activity dependent and independent manner. *Nucleic Acids Res* 45: 3503–3518.
37. Nadiminty N, et al. (2015) NF-κB2/p52:c-Myc:hnRNPA1 pathway regulates expression of androgen receptor splice variants and enzalutamide sensitivity in prostate cancer. *Mol Cancer Ther* 14:1884–1895.
38. Djusberg E, et al. (2017) High levels of the AR-V7 splice variant and co-amplification of the Golgi protein coding YIPF6 in AR amplified prostate cancer bone metastases. *Prostate* 77:625–638.